

Published in final edited form as:

*Sci Signal*. ; 4(197): ra71. doi:10.1126/scisignal.2001744.

## p53 and miRNA-34 are Suppressors of Canonical Wnt Signaling

Nam Hee Kim<sup>1,9</sup>, Hyun Sil Kim<sup>1,9</sup>, Nam-Gyun Kim<sup>2</sup>, Inhan Lee<sup>3</sup>, Hyung-Seok Choi<sup>4,8</sup>, Xiao-Yan Li<sup>5</sup>, Shi Eun Kang<sup>1</sup>, So Young Cha<sup>1</sup>, Joo Kyung Ryu<sup>1</sup>, Jung Min Na<sup>1</sup>, Changbum Park<sup>1</sup>, Kunhong Kim<sup>6</sup>, Sanghyuk Lee<sup>4,7</sup>, Barry M. Gumbiner<sup>2</sup>, Jong In Yook<sup>1,10</sup>, and Stephen J. Weiss<sup>5</sup>

<sup>1</sup>Department of Oral Pathology, Oral Cancer Research Institute, College of Dentistry Yonsei University, Seoul 120-752, Korea

<sup>2</sup>Department of Cell Biology, University of Virginia Health Sciences Center, Charlottesville, VA22908, USA

<sup>3</sup>miRcore, Ann Arbor, MI 48105, USA

<sup>4</sup>Division of Life and Pharmaceutical Sciences, Ewha Womans University, Seoul 120-750

<sup>5</sup>Division of Molecular Medicine and Genetics, Department of Internal Medicine and Life Sciences Institute, University of Michigan, Ann Arbor, MI48109, USA

<sup>6</sup>Department of Biochemistry and Molecular Biology, Brain Korea 21 Project for Medical Science of Yonsei University, Center for Chronic Metabolic Disease Research, School of Medicine, Yonsei University, Seoul 120-752, Korea

<sup>7</sup>Ewha Research Center for Systems Biology, Ewha Womans University, Seoul 120-750, Korea

### Abstract

Although loss of p53 function and activation of canonical Wnt signaling cascades are frequently coupled in cancer, the links between these two pathways remain unclear. We report here that p53 transactivates miRNA-34 (miR-34), which suppresses the transcriptional activity of  $\beta$ -catenin-T-cell factor/lymphoid enhancer factor (TCF/LEF) complexes by targeting the untranslated regions (UTRs) of a set of highly-conserved targets in a network of Wnt pathway-regulated genes. Loss of p53 function increases canonical Wnt signaling through miR-34-specific interactions with target UTRs, whereas miR-34 depletion relieves p53-mediated Wnt repression. Further, gene expression signatures reflecting the status of  $\beta$ -catenin-TCF/LEF transcriptional activity in breast cancer and pediatric neuroblastoma patients are closely associated with p53 and miR-34 functional status. Loss of p53 or miR-34 contributed to neoplastic progression by triggering the Wnt-dependent, tissue-invasive activity of colorectal cancer cells. Further, during development, miR-34 interactions with the  $\beta$ -catenin UTR determine *Xenopus* body axis polarity and Wnt-dependent gene patterning. These data provide insight into the mechanisms by which a p53-miR-34 network restrains canonical Wnt signaling cascades in developing organisms and human cancer.

<sup>10</sup>Correspondence should be addressed to J.I.Y. (jiyook@yuhs.ac) Tel: 82-2-2228-3032 Fax: 82-2-392-2959.

<sup>8</sup>Current Address: Bio & Health Group, Future IT R&D Lab., LG Electronics Inc. 221 Yangjae-Dong, Seocho-Gu, Seoul Korea 137-130

<sup>9</sup>These authors contributed equally to this work.

**Author contributions:** H.S.K., X.Y.L., K.K., S.J.W. and J.I.Y. conceived and designed the project. N.H.K., H.S.K., S.E.K., S.Y.C., J.K.R., and J.M.N. performed experiments. N.G.K. performed *Xenopus* experiments. I.L., H-S.C., C.P., & S.L. analysed bioinformatics data. H.S.K., B.M.G., J.I.Y. & S.J.W. handled project planning and wrote the paper.

**Competing interests:** I Lee is founder of the non-profit organization miRcore; there is a patent pending on the miBridge target prediction method, which is owned by the University of Michigan and exclusively licensed to miRcore. The other authors declare no competing financial interests.

## INTRODUCTION

Canonical Wnt signaling controls events ranging from cell fate determination and cell cycle regulation to cell motility and metabolism (1–7). In each case, Wnt signaling depends on the post-translational regulation of  $\beta$ -catenin levels whereby the Wnt-stabilized protein translocates to the nuclear compartment and binds to the TCF/LEF family of transcriptional co-factors (1–3, 7). In turn,  $\beta$ -catenin-TCF/LEF complexes activate transcriptional cascades that impact development (e.g., the polarity of the *Xenopus* primary body axis), the maintenance of stem cell niches in adult tissues and the induction of epithelial-mesenchymal transition (EMT) programs that characterize gastrulation, wound healing and fibrosis (1–7). In addition to the importance of the canonical Wnt pathway in normal cell function, pathologic increases in Wnt signaling are frequently implicated in neoplastic states (4–7). The importance of Wnt signaling in human cancer is highlighted by its coordinate control of the transcriptional programs underlying EMT, cancer stem cell generation and cancer progression (3–6).

In addition to the heightened levels of Wnt activity that characterizes many neoplastic states, the tumor suppressor p53 is also frequently inactivated in human cancers (8, 9); its transcriptional activity playing critical roles in maintaining its function as a tumor suppressor (10, 11). In Li-Fraumeni syndrome, an inherited disorder associated with *TP53* mutations, the age of tumor onset—especially in breast and colon cancer—directly correlates with the decrease in p53's transactivational activity (12, 13). The importance of p53 function further manifests itself in p53-null mouse models, where most mice appear normal at birth, but develop tumors at early age (14, 15). Despite the biological and clinical consequences of p53 loss of function, the mechanistic links whereby p53 suppresses oncogenic signaling remain unclear (9–13). Thus, heretofore unexplored processes may exist that allow wild type (wt) p53 to repress signaling events critical to tumorigenesis and cancer progression. Indeed, in vivo, Wnt1-overexpressing mice bred into a p53-deficient background develop mammary adenocarcinomas at an earlier age, with higher rates of tumor incidence and accelerated tumor growth relative to Wnt1 transgenic mice with wt p53-function (16–18), suggesting that p53 may act upstream of Wnt to suppress its oncogenic activity.

MicroRNAs (miRNAs) are small, non-coding RNAs that interact with complementary or near complementary target sites in the untranslated regions (UTRs) of mRNA targets, thereby repressing gene expression post-transcriptionally (19, 20). The miRNA-to-mRNA interactions form complex regulatory networks whose effects appear to be more pervasive than previously appreciated with vertebrate miRNAs affecting early embryonic development as well as tumorigenesis and metastasis (19–27). Although recent studies have demonstrated that miR-8 in *Drosophila* or miR-203 in zebrafish inhibit Wnt during development, in part by targeting *wntless*—a gene required for Wnt secretion—and LEF1, respectively (28, 29), little is known regarding the ability of miRNAs to modulate the canonical Wnt cascade.

Transcription of the evolutionarily-conserved miR-34 family falls under the direct control of p53 (30–33). Further, in many types of sporadic and hereditary cancers, the miR-34 family is silenced not only by functional inactivation of p53, but also by its chromosomal deletion or epigenetic silencing (34–39), raising the possibility that miR-34 constitutes an important arm of the p53 network. Here, we demonstrate a direct link from p53 activity and miR-34 to the canonical Wnt signaling pathways operative in development and cancer.

## RESULTS

### Tumor suppressor p53 and miR-34 inhibit Wnt activity

Supporting the hypothesis that p53 represses Wnt signaling, loss of wt-p53 increased the abundance of endogenous  $\beta$ -catenin and potentiated TOPflash activity (a reporter construct that monitors  $\beta$ -catenin-TCF/LEF transcriptional activity) in p53<sup>flox/flox</sup> mouse embryonic fibroblasts (MEFs) as well as in 293 cells (Fig. 1A and fig. S1A). Because amounts of  $\beta$ -catenin and TCF/LEF activity are co-regulated (1), we examined the abundance of upstream Wnt genes as a function of p53 status. Stable knock-down of wt-p53 increased not only  $\beta$ -catenin abundance, but also that of WNT1 and its co-receptor, low-density lipoprotein receptor-related protein 6 (LRP6), in both A549 lung cancer cells and MCF-7 breast cancer cells (Fig. 1B). Loss of p53 function induced by i) siRNA-mediated knock-down, ii) stable transduction with a human papilloma virus-E6 open reading frame (ORF), or iii) expression of mutant p53 elicited similar effects (fig. S1B and C), suggesting that p53 represses canonical Wnt signaling at multiple levels. Multiple Wnt target genes directly downstream of  $\beta$ -catenin, including CD44, MMP-7 and MYCN, showed increased mRNA expression following p53 knockdown (fig. S2A), supporting an upstream suppressor function for p53. To determine the effect of p53 loss of function on Wnt signaling in clinical samples, we analyzed a publicly available gene-expression data set of 251 breast cancer patients (40). In this dataset, the functional and mutational status of p53 had been analyzed in terms of its transcriptional function (see Methods for details regarding the p53 status of the patient dataset). We independently validated the transcriptional activity of p53 in this breast cancer cohort by analyzing transcript abundance of p53 target genes (fig. S2B). To assess potential associations between p53 status and Wnt activity in these patients, the mRNA expression of TCF/LEF target genes was examined (4, 41). In an unsupervised hierarchical analysis, the TCF/LEF gene signature in breast cancer clearly identified two distinct functional as well as mutational p53 subsets (Fig. 1C). As the mRNA expression of the TCF/LEF gene set associated with loss of p53 function, these data support the contention that canonical Wnt activity is linked to p53 status in primary breast cancer tissues.

Because the tumor suppressor role of p53 derives primarily from its transcriptional activity (10), we used p53<sup>-/-</sup> MEFs to determine the role of p53-mediated transcription on Wnt repression. As expected, both cellular  $\beta$ -catenin abundance and TOPflash activity fell significantly following stable transduction of wt-p53 into p53-null MEFs (Fig. 2A). In contrast to wt p53, neither mutant p53 with a deleted N-terminal transcriptional activation domain (dTAD) nor transcriptionally-inactive p53 mutants (R175H, R273H) suppressed Wnt activity, indicating that p53's transcriptional function is required for Wnt repression. Because the miR-34 family is a direct transcriptional target of p53 (30–33), we examined miR-34 abundance in conjunction with p53 status (Fig. 2B and fig. S3A). An inverse correlation between Wnt activity and miR-34 abundance was identified, leading us to postulate that p53 represses canonical Wnt signaling through the transcriptional activation of miR-34. Indeed, TOPflash activity was suppressed in HEK (human embryonic kidney) 293 cells by exogenous miR-34, whereas its activity was enhanced when endogenous miR-34 was depleted (Fig. 2C); similarly, p53 and miR-34 limited Wnt signaling in MEFs even in the presence of exogenous Wnt (fig. S3B to D).

Tumor suppressive miRNA genes are frequently located at fragile sites in chromosomes (36). Because loss of chromosome 1p and 11q are common in various primary cancers, especially pediatric neuroblastoma and glioma, and these deletions encompass the coding regions for miR-34a and miR-34b/c respectively, we hypothesized that these deletions combined with microarray dataset might serve as a miR-loss platform in human cancer tissues (42). To assess the repressor function of miR-34 on Wnt activity in clinical samples, a microarray gene expression data set with relevant chromosomal information was used

from a study of pediatric neuroblastoma patients (see Methods for detailed information) (42, 43). In an unsupervised analysis, TCF/LEF gene signatures successfully identified miR-34 status based on chromosome 1p and 11q deletions (Fig. 2D and fig. S3E). Thus, the expression of genes activated downstream of TCF/LEF was specifically increased in samples from patients with tumors showing 1p-loss or 11q-loss, consistent with the proposed roles for miR-34 family members as repressors of Wnt signaling.

### Canonical Wnt genes are direct targets of miR-34

To determine whether miR-34 constitutes an inhibitory arm of the Wnt cascade, we next investigated various putative miR-34 targets and interaction sites using the miBridge target class, an algorithm for specific miR-mRNA binding predictions (44). Potential binding sites for miR-34a, miR-34b\*, and miR-34c-5p were identified in the UTRs of not only  $\beta$ -catenin, WNT1, and LRP6, but also in those of WNT3 and LEF1 (Fig. 3A, Table S1 and S2). Furthermore, miR-34 family member sequences (Table S3) and potential miR-34 mRNA binding sites (Table S4) were highly conserved in vertebrates, including various mammals as well as birds (identified in *Gallus*) and amphibia (identified in *Xenopus*). To determine whether miR-34 represses these Wnt pathway genes through their respective UTRs, we cloned the UTRs of human WNT1, WNT3, LRP6,  $\beta$ -catenin and LEF1 downstream of luciferase reporter constructs, transfected them in A549 or MCF-7 cells, and assessed the effects of miR-34 on luciferase activity. Transduction with expression vectors encoding either miR-34 family members or synthetic miR-34a decreased the activities of the UTR reporter genes relative to that of control luciferase without a cloned UTR (Fig. 3B, fig. S4A and B). Mutation of putative miR-binding sites in the WNT1, WNT3 or  $\beta$ -catenin UTRs abolished the repressor function of miR-34 (fig. S4C). Similarly, the abundance of WNT1, LRP6, and  $\beta$ -catenin transcripts and proteins was also decreased by miR-34a (Fig. 3C, fig. S4D). To determine whether the putative miR binding sites contributed to miR-34-mediated inhibition of Wnt target genes, we constructed flag-tagged expression vectors of wt- $\beta$ -catenin with either no UTR or UTRs of varying length so as to include 0, 2, 3 or 4 of the predicted binding sites. Co-expression of exogenous miR-34a decreased the abundance of these  $\beta$ -catenin constructs in proportion to the number of putative target sites, but failed to affect the abundance of the construct lacking the UTR (Fig. 3D).

### Endogenous miR-34 mediates repression of canonical Wnt signaling by p53

We next examined the role of endogenous miR-34 in regulating Wnt activity in two carcinoma cells that retain wt-p53 activity (A549 and MCF-7 cells). Functional inhibition of miR-34a, the most abundant member of the miR-34 family, with complementary RNA increased the activity of a Wnt UTR reporter in both cell lines (Fig. 4A and fig. S4E), but not that of the reporters in which the UTRs contained mutant miR-34 binding sites (Fig. 4B). Furthermore, depletion of functional miR-34a not only increased the expression of WNT1, LRP6 and  $\beta$ -catenin mRNA in A549 or MCF-7 cells (Fig. 4C, fig. S4E and F), but also increased that of known  $\beta$ -catenin target genes (Fig. 4D). Moreover, the protein abundance of  $\beta$ -catenin encoded by expression vectors with UTRs of varying length was decreased in proportion to the number of target sites in the UTR and this was reversed when endogenous miR-34a function was inhibited (Fig. 4E).

Next, Wnt gene UTR reporter activities in A549 or MCF-7 cells was examined following knock-down of wt-p53. Following stable or transient knock-down of wt-p53, the activities of the Wnt gene UTR reporters increased, whereas pri-miR-34 transcription and mature miR-34a abundance decreased (Fig. 4F and fig. S5). Under physiologic conditions, the E3 ubiquitin ligase of MDM2 (murine double minute 2) acts to limit the abundance of wt-p53 (9, 10). Treatment of A549 or MCF-7 cells with an MDM2 inhibitor, Nutlin-3, decreased Wnt abundance and the activity of the Wnt gene UTR reporter, but increased pri-miR-34

abundance (fig. S6). To further verify the role of miR-34 in p53-mediated inhibition of Wnt, a miR-34a inducible system was constructed in cells in which endogenous p53 was knocked down with a specific shRNA. As expected, p53 knock-down decreased miR-34 expression, resulting in increased  $\beta$ -catenin abundance and  $\beta$ -catenin UTR gene reporter activity (Fig. 4G and H). The effects of p53 knock-down were largely relieved by induction of miR-34 with doxycycline (Fig. 4G and H). Similarly, in a p53-null background, Wnt activity was inhibited following the expression of wt-p53, and restored following miR-34a silencing (Fig. 5A and B, fig. S6C), indicating that p53-mediated inhibition of Wnt is mainly attributable to miR-34. Because p53 can directly or indirectly increase the abundance of multiple miRNAs (32), it remained possible that additional miRNAs regulated by p53 could also inhibit Wnt activity. To investigate this possibility, we tested the effects of several intergenic miRNAs, including miR-27, miR-30, and miR-192, that are known to be upregulated by p53 on Wnt activity (32). Following transfection of each of these miRNAs in cells co-expressing Wnt UTR reporters or TOPflash, only miR-34 decreased the UTR reporter and TOPflash activities, although the other miRNAs inhibited their respective control targets (Fig. 5C and D).

We further compared an expression signature responsive to miR-34 in *Dicer*<sup>-/-</sup> cells (32) to clinical samples to determine whether an analysis of miR-34 gene targets could strengthen evidence for the link between p53 activity and canonical Wnt signaling. Indeed, changes in gene expression predicted to occur in response to low miR-34 activity (i.e., increased expression of miR-34-responsive genes) clearly associated with sample subsets displaying high TCF/LEF gene signatures, mutant p53 function in the breast cancer cohort and with subsets of chromosome 1p loss in the neuroblastoma dataset, respectively (Fig. 5E). Hence, miR-34 functionally links p53 and Wnt signaling in affected patient samples.

### miR-34 suppresses Wnt activity during *Xenopus* development

Although physiological and developmental functions of p53 in *Xenopus* have not been clearly defined (45), the aberrant duplication of the embryonic axis in early *Xenopus* embryos is controlled by Wnt and  $\beta$ -catenin signaling (2, 46). Because miR-34 and its binding sites in the  $\beta$ -catenin UTR are highly conserved in vertebrates, and the effect of  $\beta$ -catenin on stimulating TCF/LEF transcriptional activity largely depends on interactions between its UTR and miR-34 (Fig. 6A), we tested the hypothesis that these miR-UTR interactions play a role in limiting  $\beta$ -catenin activity in *Xenopus* development. When  $\beta$ -catenin mRNA lacking its UTR was injected into the *Xenopus* ventral blastomere, axis duplication was observed in more than 70% of the embryos, whereas  $\beta$ -catenin constructs containing 790 bp of the UTR induced axis duplication in less than 10% of the embryos (Fig. 6B). UTR-dependent repression of  $\beta$ -catenin function, as assessed by either TOPflash activity or axis duplication, was abolished by mutating putative miR-34 target sites (Fig. 6C and D), indicating that miR-UTR interactions regulate  $\beta$ -catenin function in *Xenopus* development. Furthermore, injection of miR-34 into the ventral blastomeres of *Xenopus* embryos blocked Wnt-induced axis duplication (Fig. 6E). Because injection of anti-miR-34 into the ventral marginal zone (n=18) or dorsal marginal zone (n=17) of *Xenopus* embryos induced embryonic lethality by the end of gastrulation whereas injection of a negative control did not (n=20), we chose a cap explant assay with the animal pole of blastomeres to investigate the role of endogenous miR-34 in limiting signaling through the Wnt/ $\beta$ -catenin pathway. Indeed, in a fashion similar to that observed following the application of exogenous Wnt, depletion of endogenous miR-34 increased mRNA expression for the Wnt- $\beta$ -catenin-responsive patterning genes *Siamois*, *Xnr3*, and *Chordin* (Fig. 6F). In contrast, the addition of exogenous precursors of miR-34a decreased the expression of these patterning genes (Fig. 6F). Thus, as observed in human cancer tissues, miR-34 also inhibits Wnt signaling during *Xenopus* development (Fig. 6G).

## Hyperactivation of the canonical Wnt signaling pathway following loss of p53-miR-34 function contributes to cancer progression

Mutations in APC (adenomatous polyposis coli) or  $\beta$ -catenin that lead to constitutive activation of the canonical Wnt signaling pathway are key steps in initiating colorectal tumorigenesis (47). In the multistep progression of colorectal cancer, loss of wt-p53 function tends to occur relatively late in the disease process, during the transition from adenoma to invasive colorectal carcinoma (48). To investigate the gatekeeper role of the p53-miR-34 axis in regulating constitutive Wnt signaling in cancer, we used LoVo and SNU-81 colon carcinoma cells, which express mutant APC, but retain wt-p53 function. In these cells, either p53 knock-down or miR-34 silencing increased Wnt signaling without affecting mutant APC abundances (Fig. 7A and fig. S7A). In SW480 and SW620 colon carcinoma cells, which carry mutations in both APC and p53, transduction of miR-34a decreased  $\beta$ -catenin abundance and inhibited Wnt1, LRP6,  $\beta$ -catenin UTR activities (Fig. 7B). TOPflash activity, which was inhibited by wt-APC or miR-34 alone, was further inhibited when wt-APC and miR-34 were co-expressed (Fig. 7B). By contrast the p53-miR-34 axis remained functional in HCT116 and SNU-407 colon carcinoma cells that express mutant  $\beta$ -catenin but retain wt-p53 function (fig. S7B). To further assess the role of miR-34 in colorectal cancer progression, invasion assays were performed using the live chick chorioallantoic membrane (CAM), which provides an in vivo system for monitoring the ability of cancer cells to traverse an intact basement membrane and infiltrate underlying interstitial tissues (5, 6, 49). As predicted, the invasive activity of p53-mutant SW480 and SW620 cells was largely blocked in vivo when miR-34a abundance was increased, and the CAM basement membrane was preserved (Fig. 7C). Furthermore, the anti-invasive effects of miR-34a depended on its interaction with the intact  $\beta$ -catenin UTR (fig. S8). Together, these data support the hypothesis that miR-34 counterbalances the effects of APC or  $\beta$ -catenin mutations in the early stages of colorectal tumorigenesis (48, 50), and that the hyperactive Wnt signaling program that accompanies malignant progression likely results as a consequence of the combined loss of p53 and miR-34 function.

## DISCUSSION

Here, we have demonstrated that the miR-34 family links p53 activity with the canonical Wnt pathway through miR-34-specific interactions with the UTRs of multiple Wnt pathway genes, and thereby to the inhibition of  $\beta$ -catenin-TCF/LEF-dependent transcriptional activity. The UTRs of proto-oncogenes, including  $\beta$ -catenin, are often shortened in cancer cells as a consequence of alternative cleavage and polyadenylation; resulting in both enhanced mRNA stability and heightened transforming activity (51, 52). Our findings, in conjunction with these and other studies, suggest that the loss of normal regulatory interactions between tumor suppressor miR-34 family members and their target UTRs in genes associated with canonical Wnt pathway can lead to a sustained amplification of oncogenic signaling (21). In addition, the activation of Wnt signaling that occurs as a consequence of the loss of p53 and miR-34 function may provide a genetic basis for the developmental defects and cancer-prone status of p53-mutant mice (14, 15, 53). Because p53-miR-34 targets such as LRP6 have also been implicated in G-protein coupled receptor signaling (54, 55), the regulatory function of the p53-miR-34 axis likely extends beyond development and neoplasia alone.

Although our findings establish a direct link between the p53-miR-34 axis and WNT1, LRP6,  $\beta$ -catenin and LEF-1 expression, additional Wnt-related genes targets of the p53-miR-34 axis are probably affected. For example, increases in the abundance of WNT1 and AXIN2, two miR-34 targets (44, 56), stabilize nuclear abundance of the transcriptional repressor, Snail1, thereby triggering a tissue-invasive phenotype in cancer cells by promoting EMT (6, 49, 57). Although we were unable to identify Wnt repressor functions

among the intergenic miRNAs, miR-27, miR-30, or miR-192 (32), other p53-regulated miRNAs may work in tandem with miR-34. For example, recent reports have linked p53 to the regulation of miR-200 family members (58). In human cancers, the miR-200 family has also been characterized as an EMT suppressor due to its targeting of the E-cadherin repressors, zinc finger E-box binding homeobox 1 (ZEB1) and ZEB2 (24, 59). miR-200 also targets the UTR of  $\beta$ -catenin (60), though the functional outcomes of this regulation are unknown. Nevertheless, we speculate that miR-34 and miR-200 family members coordinately regulate Wnt signaling in response to changes in p53 activity.

The tumor suppressor function of p53 in bona fide oncogenic signaling events, such as those linked to *MYC*, *RAS*, and *E1A* have long been noted (8, 61), but direct molecular links between the transcriptional activity of p53 and oncogenic transformation have remained largely undefined. Indeed, most of p53's downstream target genes appear to be involved in physiological processes, and loss of p53 function in vivo increases cell proliferation rather than inhibiting apoptosis (17). *MYC* orthologues are downstream target genes of canonical Wnt signaling cascades and have been identified as miR-34 targets (62, 63). Further, activation of Wnt- $\beta$ -catenin and *MYC* pathways are correlated with aggressive behavior in human cancers in terms of triggering EMT-like changes in cancer cells or promoting the adoption of cancer stem cell-like features (4, 64). Given studies implicating miR-34 and p53 in the self-renewal of cancer stem cells (25, 64), both oncogenic signaling and stem cell renewal may fall within the purview of the p53-miR-34 axis described herein.

miR-34a and miR-34b/c are located on chromosomes 1p36 and 11q23, respectively; regions in which deletions are associated with early stage cancers and with the more bleak prognoses associated with sporadic and familial cancers (34, 35, 38, 65). Furthermore, chromosomal losses in these regions are commonly found in familial malignant melanoma-dysplastic nevus syndrome, familial gliomas and pediatric neuroblastomas (34, 35, 65). Although various genes map to these sites, conventional tumor suppressors other than miR-34a and miR-34b/c have not been identified in these regions (33, 36). Loss of 1p and p53 mutation are mutually exclusive in gliomas, supporting a specific role for miR-34 in tumorigenesis (66, 67). Of note, epigenetic silencing of miR-34 by aberrant CpG methylation also occurs in various types of human cancer (37, 39). Therefore, sustained activation of Wnt signaling may arise independently of p53 mutations as a consequence of chromosomal loss or epigenetic silencing of miR-34. Thus, we propose that miR-34-dependent perturbations in the interconnected p53 and canonical Wnt pathways endow cancer cells with the ability to subvert p53-dependent tumor suppressor programs while activating the Wnt-dependent machinery that supports clonal expansion and the acquisition of the aggressive phenotypes associated with cancer progression.

## MATERIALS AND METHODS

### Cell lines and chemicals

MCF-7, A549, and 293 cells were cultured in Dulbecco's modified Eagle's medium (DMEM) supplemented with 10% fetal bovine serum (FBS) (5, 6). SW480 and SW620 cells were obtained from ATCC and cultured under in DMEM with 10% FBS. Colorectal cancer cells, LoVo and SNU-81, were obtained from the Korean Cell Line Bank. p53-null mouse embryonic fibroblasts (MEFs) were obtained from ATCC (CRL-2821) and p53 floxed mice were kindly provided by Dr. J-L Guan (University of Michigan). Primary dermal fibroblasts were obtained from mouse skin. The functional status of p53 in various cancer cell lines was confirmed through the TP53 database (<http://www-p53.iarc.fr/>). An MDM2 inhibitor, Nutlin-3 (Sigma), was dissolved in DMSO and used at a final concentration of 10  $\mu$ M. Conditioned medium for exogenous Wnt treatment was prepared from the conditioned media of Wnt3a-producing L-cells (5, 6).

## Constructs and viral transduction

Retroviral expression vector of HPV-E6 was constructed by cloning of HPV-E6 ORF (68) into a pQCXIP retroviral expression vector (Clontech). Lentiviral shRNA-dsRed-VSVG construct for p53 (69), control vector with packaging constructs, and adenovirus expressing Cre recombinase were obtained from the University of Michigan Vector Core. TOPflash (pGL3-OT), FOPflash (pGL3-OF), reporter constructs for p21 and PUMA, wild type p53 (plasmid 16434), and mutant p53 (plasmid 16346 for R175H and plasmid 16439 for R273H) expression vectors were obtained from Addgene. An expression vector for the p53 transactivation domain deletion mutant (dTAD) was generated using PCR-based methods. Wild type and mutant p53 were subcloned into pLentilox-IRES-GFP for lentiviral transduction. Flag-tagged wild type  $\beta$ -catenin, pCMV-APC, pMSCV-miR-34a, and -34b/c expression vectors were kindly provided by E. R. Fearon (University of Michigan). Adenovirus expressing GFP (ad-GFP, #1060) and GFP-p53 (ad-GFP-p53, #1260) were purchased from Vector Biolabs. p53-null MEFs were transduced with adenoviral expression vectors by directly applying the diluted viruses to the culture medium at 100 multiplicity of infection. Transduction efficiency was determined by direct visualization using fluorescent microscopy of GFP-expressing cells. All expression and reporter vectors used in this study were verified by sequencing.

## miR-34 family target screening and prediction

The miR-34 family and other miRNA sequences of various species were obtained from miRBase (<http://www.mirbase.org/index.shtml>). The initial miBridge prediction set was used to identify potential miRNAs targeting more than two Wnt signaling genes (44), one of which being either WNT1,  $\beta$ -catenin (CTNNB1), or LRP6. The parameters of this prediction algorithm include seven or more consecutive matches of Watson-Crick hybridization with an energy threshold at  $-13$  kcal/mol using RNAhybrid (<http://bibiserv.techfak.uni-bielefeld.de/rnahybrid/>). The miBridge algorithm was then modified (including GU wobbles), with the energy threshold for the 5' UTR interaction at  $-14$  kcal/mol and the 3' UTR interaction at  $-15$  kcal/mol to predict additional targets among the initially screened miRNAs. Additional targets were predicted through the miRcore service (<http://mircore.org>). The identified 3' UTR interaction sites were compared with TargetScan and Pictar targets and checked for conservation using the UCSC Genome Browser (<http://genome.ucsc.edu/>).

## UTR Reporter assays and miRNA constructs

A luciferase expression construct with multiple cloning sites for UTRs was used as described previously (44). The 3'-UTRs of WNT1 (NM\_005430; +1 ~ +920), WNT3 (NM\_030753; +1 ~ +151),  $\beta$ -catenin (NM\_001904; +1 ~ +1157), and LEF1 (NM\_016269; +6 ~ +712) were amplified from genomic DNA of MCF-7 cells and subcloned into the *Bam*HI and *Not*I sites downstream of luciferase. For the UTR of LRP6 (NM\_002336), the UTR reporter of LRP6-1 (+1 ~ +230) and of LRP6-2 (+1036 ~ +2401) were generated using the same method. The miRNA expression vectors for miR-27a ( $-296$  ~ +235), miR-30a ( $-358$  ~ +197), miR-98 ( $-354$  ~ +199), and miR-192 ( $-321$  ~ +213) were constructed from PCR-amplified products obtained from the genomic DNA of MCF-7 cells followed by subcloning into the pLPCX vector (Clontech). As a positive control reporter for miRNAs, synthetic oligonucleotides of complementary sequences for each miRNA were hybridized and inserted into *Not*I and *Xba*I sites downstream of luciferase.  $\beta$ -catenin expression vectors in which the UTR was serially deleted or retained were constructed by substituting Flag-tagged  $\beta$ -catenin cDNA for firefly luciferase in a control luciferase vector ( $\beta$ -catenin-CDS) or a  $\beta$ -catenin UTR reporter construct following serial deletion of the UTR by PCR ( $\beta$ -catenin-CDS-UTR-nt +1~+170, -nt 1~480, -nt -1~790). Mutant UTR reporter constructs were constructed by deletion of the seed-matched portion of the potential target

sites of Wnt1, Wnt3, and  $\beta$ -catenin (1–170). Cells were co-transfected with each of the UTR reporter constructs (2–100 ng) and miR-34 family expression vectors (200–500 ng) or synthetic miRNA (Ambion) as indicated. As a transfection control, 1 ng of SV-40-*Renilla* construct (Promega) was co-transfected with the reporter vectors. For functional analyses of miRNA precursors, 20 nM of miR-34 (PM11030) or a negative control (AM17110) were transfected with lipofectamine 2000 (Invitrogen). For functional inhibition of endogenous miRNA, cells were treated with anti-miR-34a inhibitor (AM11030) or a negative control (AM17010) a total of two times at 2 d intervals. Cells were lysed 48h after transfection and the relative ratio of *Renilla* to firefly luciferase was determined by dual luciferase assay (Promega). All reporter assays were performed in triplicate.

### Microarray data analysis of clinical samples

Publicly available gene expression data from the Uppsala breast cancer cohort (GSE3494, raw data) and a primary neuroblastoma series (GSE13141, processed by GCOS 1.1.1 and normalized using GeneSpring GX) using HG-U133A Plus 2.0 arrays were downloaded from the Gene Expression Omnibus (40, 43). The functional status of p53 DLDA (diagonal linear discriminant analysis) classifier as well as mutational status of p53 cDNA for 251 breast cancer patients was also obtained from GSE3494. The breast cancer dataset consists of 193 cases expressing wild-type p53 and 58 cases harboring p53 mutations, representing 179 cases of wild type DLDA function and 72 cases of mutant p53 function (40). The dataset for 30 cases of pediatric neuroblastoma samples is comprised of 12 cases of chromosome 1p deletion and 6 cases of 11q deletion. Genes regulated by TCF/LEF and miR-34a were obtained from independently published results (32, 41) and matched to the corresponding Affymetrix probes. The TCF/LEF signature consisted of 132 probes (U133A Affymetrix chip) of 74 genes that were responsive to dominant-negative TCF4 (2 fold cut-off) in colon cancer cells (41), and a miR-34a signature consisting of 56 probes (U133A Affymetrix chip) that were downregulated by miR-34a expression in HCT116 Dicer<sup>EX5</sup> cells (GSE7864) (32). The probe ID and gene list are listed in Table S5. The raw breast cancer data were normalized with the Robust Multichip Average (RMA) as implemented in the “rma” function in the R Bioconductor “affy” package. For an unsupervised hierarchical cluster analysis of TCF/LEF or miR-34 responsive genes, Ward linkage method was used together with the Pearson distance (breast cancer samples) or the Euclidean distance (neuroblastoma samples) for both sample and gene clustering. The statistical significance of the association between the hierarchical clusters of TCF/LEF genes and p53 groups of breast cancer, or between the clusters and 1p/11q deletion of neuroblastoma were determined by two-tailed Fisher’s exact test. Patient subgroups with high and low TCF/LEF activity, as determined by the hierarchical clustering, were used to assess the statistical association between hierarchical clusters of miR-34 genes and TCF/LEF subgroups, as well as the association between the clusters and p53/1p status. To validate the functional status of p53 in breast cancer samples, the transcript expression levels of known p53 target genes were compared relative to the p53 status, and the differences in transcript levels determined by one-sided *t*-test. The list of p53 downstream target genes was obtained from previously published results (11).

### Xenopus axis duplication and animal cap assay

*Xenopus laevis* eggs were fertilized, de-jellied and incubated in 0.1 × Modified Barth’s Solution (1 × MBS: 88 mM NaCl, 1 mM KCl, 0.7 mM CaCl<sub>2</sub> 1 mM MgSO<sub>4</sub> 5 mM HEPES pH 7.8, and 2.5 mM NaHCO<sub>3</sub>). For the axis duplication assay,  $\beta$ -catenin mRNA (5pg/nL) without its UTR, with various sized UTRs, or with mutant UTRs synthesized with the Riboprobe system (Promega) were injected into one of the ventral vegetal blastomeres of 4- to 8-cell-stage embryos. The embryos were then allowed to develop at room temperature in 0.1 × MBS and axis duplication was scored at the tadpole stage. For axis duplication with

Wnt8, 30 pg of Wnt8 mRNAs were co-injected with 0.4 pmol of control miRNA or miR-34 into one of the ventral vegetal blastomeres of 4- to 8-cell-stage *Xenopus* embryos. Embryos were scored in three categories: complete secondary axis, partial secondary axis (small posterior protrusion or pigmented spot/line), and normal single axis. For the animal cap assay, each blastomere of the *Xenopus laevis* 2-cell-stage embryo was injected with 5 nL either of control miRNA (40  $\mu$ M), miR-34a (40  $\mu$ M), anti-miR-34a (20  $\mu$ M), or 50 pg of Wnt8 mRNA in the animal pole region, and cultured at 16 °C in 0.1  $\times$  MBS buffer. Animal caps of embryos were dissected from blastula stage embryos (stage 8.5 – 9) and cultured in 0.5x MBS buffer for 2–4 hours until gastrula stage (stage 10.5). RT-PCR was performed on total RNA isolated from the animal caps with Trizol (Invitrogen). Oligonucleotide sequences used for the RT-PCR analyses in this study are shown in Table S6.

### Generation of Stable Transfectant Cells and Tet-inducible miR-34a Cells

pQCXIP-HPV-E6 expression or control vector were used to generate retroviral stocks in HEK293 cells for subsequent infection of MCF-7 or A549 cells. Stable HPV-E6 transfectants were obtained following selection with 1.0  $\mu$ g/ml of puromycin. For stable knock-down of p53, each cell line was transduced using lentiviral shRNA for p53 or control vector. Stable knockdown of p53 by HPV-E6 or shRNA was confirmed by Western blot analysis. A primary transcript sequence from pMSCV-miR-34a vector was subcloned into episomal doxycycline-inducible expression vector (6). MCF-7 cells were then transduced with episomal miR-34a expression vector and selected with hygromycin (200  $\mu$ g/ml). The Tet-inducible cells were maintained in Tet-free condition, and doxycycline was directly added to Tet-free culture medium at the indicated concentrations for miR-34a induction.

### RT-PCR and immunoblot analysis

Conventional reverse transcriptase with random hexamers was used for synthesis of cDNA for primary transcripts of human and mouse miR-34a and miR-34b/c. Primer3 software was used to design the primers to amplify the miR-34 family pri-miRNA and the control GAPDH. PCR reactions were performed for miR-34a (30 cycles) and miR-34b/c (34 cycles) and annealed at 57 °C. The amplified product was visualized by UV illuminator and then cloned into TA-vector to verify the sequence of the PCR products. Real-time qPCR analysis for pri-miR-34a and proven  $\beta$ -catenin target genes was performed using an ABI-7300 instrument under standard conditions and SBGR mix ( $n = 3$ ). The list of 13 direct target genes of  $\beta$ -catenin was obtained from the Nusse homepage (<http://www.stanford.edu/~rnusse/wntwindow.html>). The expression of  $\Delta$ Ct value from each sample was calculated by normalizing with GAPDH. Primer specificity and PCR reaction were verified by dissociation curve after PCR reaction. For quantitative analysis of mature miR-34a levels, human TaqMan miRNA assay kits (Applied Biosystems, assay ID 000426 for miR-34a, ID 001001 for *RNU24*, and ID001973 for *U6 snRNA*) were used for reverse transcription with specific primers, and qPCR was performed with corresponding probes ( $n = 3$ ). The expression of mature miR-34a  $\Delta$ Ct values from each sample were calculated by normalizing with RNU24 or U6 expression values. Conservation of UTR and miR-34 target sites in  $\beta$ -catenin mRNA in HCT116 and SNU-407 cells were confirmed by RT-PCR and sequence analysis. siRNA oligo duplexes for negative control and p53 were purchased from Santa Cruz. The specificity of antibodies for WNT1 and LRP6 detection was determined with HA-tagged expression vectors (fig. S1D). Truncated APC in colon cancer cells was detected by Western blot and the corresponding molecular weight. To detect endogenous protein expression, total cell lysates in Triton X-100 buffer (20  $\mu$ g for LRP6, WNT1, and APC; 1–2  $\mu$ g for p53, and  $\beta$ -catenin) were subjected to SDS-PAGE and immunoblotting. Antibodies directed against LRP6 (C5C7, #2560, Cell Signaling Technology), WNT1 (ab63934, Abcam),  $\beta$ -catenin (610154, BD Bioscience), APC (H-290,

Santa Cruz), M2 mAb flag-tag (Sigma), p53 (DO-1 or pAb240, Santa Cruz, and tubulin (Labfrontier, Korea) were obtained from the commercial vendors.

### Chick chorioallantoic membrane (CAM) invasion assay

Non-invasive, dsRed-expressing SW480 or SW620 cells transfected with negative control or miR-34a were labeled with fluoresbrite carboxylate nanospheres (Polysciences, Inc., Warrington, PA). The colon cancer cells were cultured on the CAM of 11-day-old chick embryos for 3 days as described previously (5, 6, 49). Type IV collagen staining of frozen CAM sections was performed with a chick-specific monoclonal antibody (IIB12) (5) and Alexa-Fluor-labeled secondary antibodies. Invasion was monitored in cross-sections of the fixed CAM by fluorescent microscopy as described (5, 6, 49). DAPI (Molecular Probes) was used to stain cell nuclei.

### Statistical Analysis

Statistical significance of reporter assays and quantitative PCR were determined by the Student's *t* test. Differences were considered significant when the *P* value was less than 0.05 or 0.01 as indicated in the text. The statistical significance of *Xenopus* axis duplication was determined by binomial *t* test for single axis embryos.

### Supplementary Material

Refer to Web version on PubMed Central for supplementary material.

### Acknowledgments

We thank Y. S. Lee for critical reading of the manuscript, and also wish to thank Eph Tunkle and Y. H. Cha for preparation of the manuscript. We thank Y-M Huh for supervising microarray data analysis. E. R. Fearon and G. T. Bommer generously provided constructs and cell lines along with helpful discussion.

**Funding:** This study was supported by a grant from the National R&D Program for Cancer Control (0720270 and 1020110), a grant from the Korea Health Technology (A080916 and A084699), Ministry of Health & Welfare, a grant from the National Research Foundation of Korea (NRF) funded by the Korea government (MEST) (2011-0000358, 2011-0002620, 2010-0029703, R15-2004-024-00000-0), Korea Research Institute of Chemical Technology (SI-1105), and a grant from the BioGreen 21 program of the Korean Rural Development Administration (20070401034010). This work is also supported by National Institutes of Health (NIH) grant R37 GM037432 (B.M.G), CA116516 (S.J.W) and the Breast Cancer Research Foundation (S.J.W). The funding agencies had no role in study design, data collection and analysis, decision to publish, or preparation of the manuscript.

### REFERENCES AND NOTES

1. Grigoryan T, Wend P, Klaus A, Birchmeier W. Deciphering the function of canonical Wnt signals in development and disease: conditional loss- and gain-of-function mutations of beta-catenin in mice. *Genes Dev.* 2008; 22:2308–2341. [PubMed: 18765787]
2. Petersen CP, Reddien PW. Wnt signaling and the polarity of the primary body axis. *Cell.* 2009; 139:1056–1068. [PubMed: 20005801]
3. Nelson WJ, Nusse R. Convergence of Wnt,  $\beta$ -catenin, and cadherin pathways. *Science.* 2004; 303:1483–1487. [PubMed: 15001769]
4. Nguyen DX, Chiang AC, Zhang XH, Kim JY, Kris MG, Ladanyi M, Gerald WL, Massague J. WNT/TCF signaling through LEF1 and HOXB9 mediates lung adenocarcinoma metastasis. *Cell.* 2009; 138:51–62. [PubMed: 19576624]
5. Yook JI, Li XY, Ota I, Fearon ER, Weiss SJ. Wnt-dependent regulation of the E-cadherin repressor snail. *J. Biol. Chem.* 2005; 280:11740–11748. [PubMed: 15647282]

6. Yook JI, Li X-Y, Ota I, Hu C, Kim HS, Kim NH, Cha SY, Ryu JK, Choi YJ, Kim J, Fearon ER, Weiss SJ. A Wnt-Axin2-GSK3 $\beta$  cascade regulates Snail1 activity in breast cancer cells. *Nat. Cell Biol.* 2006; 8:1398–1406. [PubMed: 17072303]
7. Logan CY, Nusse R. The Wnt signaling pathway in development and disease. *Annu. Rev. Cell Dev. Biol.* 2004; 20:781–810. [PubMed: 15473860]
8. Finlay CA, Hinds PW, Levine AJ. The p53 proto-oncogene can act as a suppressor of transformation. *Cell.* 1989; 57:1083–1093. [PubMed: 2525423]
9. Levine AJ, Hu W, Feng Z. The P53 pathway: what questions remain to be explored? *Cell Death Differ.* 2006; 13:1027–1036. [PubMed: 16557269]
10. Riley T, Sontag E, Chen P, Levine A. Transcriptional control of human p53-regulated genes. *Nat. Rev. Mol. Cell Biol.* 2008; 9:402–412. [PubMed: 18431400]
11. Wei C-L, Wu Q, Vega VB, Chiu KP, Ng P, Zhang T, Shahab A, Yong HC, Fu Y, Weng Z, Liu JJ, Zhao XD, Chew J-L, Lee YL, Kuznetsov VA, Sung W-K, Miller LD, Lim B, Liu ET, Yu Q, Ng H-H, Ruan Y. A global map of p53 transcription-factor binding sites in the human genome. *Cell.* 2006; 124:207–219. [PubMed: 16413492]
12. Petitjean A, Achatz MI, Borresen-Dale AL, Hainaut P, Olivier M. TP53 mutations in human cancers: functional selection and impact on cancer prognosis and outcomes. *Oncogene.* 2007; 26:2157–2165. [PubMed: 17401424]
13. Olivier M, Goldgar DE, Sodha N, Ohgaki H, Kleihues P, Hainaut P, Eeles RA. Li-Fraumeni and related syndromes: correlation between tumor type, family structure, and TP53 genotype. *Cancer Res.* 2003; 63:6643–6650. [PubMed: 14583457]
14. Donehower LA, Harvey M, Slagle BL, McArthur MJ, Montgomery CA Jr, Butel JS, Bradley A. Mice deficient for p53 are developmentally normal but susceptible to spontaneous tumours. *Nature.* 1992; 356:215–221. [PubMed: 1552940]
15. Donehower LA, Lozano G. 20 years studying p53 functions in genetically engineered mice. *Nat. Rev. Cancer.* 2009; 9:831–841. [PubMed: 19776746]
16. Donehower LA, Godley LA, Aldaz CM, Pyle R, Shi YP, Pinkel D, Gray J, Bradley A, Medina D, Varmus HE. Deficiency of p53 accelerates mammary tumorigenesis in Wnt-1 transgenic mice and promotes chromosomal instability. *Genes Dev.* 1995; 9:882–895. [PubMed: 7705663]
17. Jones JM, Attardi L, Godley LA, Laucirica R, Medina D, Jacks T, Varmus HE, Donehower LA. Absence of p53 in a mouse mammary tumor model promotes tumor cell proliferation without affecting apoptosis. *Cell Growth Differ.* 1997; 8:829–838. [PubMed: 9269892]
18. Gunther EJ, Moody SE, Belka GK, Hahn KT, Innocent N, Dugan KD, Cardiff RD, Chodosh LA. Impact of p53 loss on reversal and recurrence of conditional Wnt-induced tumorigenesis. *Genes Dev.* 2003; 17:488–501. [PubMed: 12600942]
19. Bartel DP. MicroRNAs: genomics, biogenesis, mechanism, and function. *Cell.* 2004; 116:281–297. [PubMed: 14744438]
20. Kim VN. MicroRNA biogenesis: coordinated cropping and dicing. *Nat. Rev. Mol. Cell Biol.* 2005; 6:376–385. [PubMed: 15852042]
21. Kumar MS, Lu J, Mercer KL, Golub TR, Jacks T. Impaired microRNA processing enhances cellular transformation and tumorigenesis. *Nat. Genet.* 2007; 39:673–677. [PubMed: 17401365]
22. Lee YS, Dutta A. MicroRNAs in cancer. *Annu. Rev. Pathol.* 2009; 4:199–227. [PubMed: 18817506]
23. Flynt AS, Li N, Thatcher EJ, Solnica-Krezel L, Patton JG. Zebrafish miR-214 modulates Hedgehog signaling to specify muscle cell fate. *Nat. Genet.* 2007; 39:259–263. [PubMed: 17220889]
24. Gregory PA, Bert AG, Paterson EL, Barry SC, Tsykin A, Farshid G, Vadas MA, Khew-Goodall Y, Goodall GJ. The miR-200 family and miR-205 regulate epithelial to mesenchymal transition by targeting ZEB1 and SIP1. *Nat. Cell Biol.* 2008; 10:593–601. [PubMed: 18376396]
25. Ji Q, Hao X, Zhang M, Tang W, Yang M, Li L, Xiang D, Desano JT, Bommer GT, Fan D, Fearon ER, Lawrence TS, Xu L. MicroRNA miR-34 inhibits human pancreatic cancer tumor-initiating cells. *PLoS One.* 2009; 4:e6816. [PubMed: 19714243]

26. Martello G, Zacchigna L, Inui M, Montagner M, Adorno M, Mamidi A, Morsut L, Soligo S, Tran U, Dupont S, Cordenonsi M, Wessely O, Piccolo S. MicroRNA control of Nodal signalling. *Nature*. 2007; 449:183–188. [PubMed: 17728715]
27. Xu N, Papagiannakopoulos T, Pan G, Thomson JA, Kosik KS. MicroRNA-145 regulates OCT4, SOX2, and KLF4 and represses pluripotency in human embryonic stem cells. *Cell*. 2009; 137:647–658. [PubMed: 19409607]
28. Kennell JA, Gerin I, MacDougald OA, Cadigan KM. The microRNA miR-8 is a conserved negative regulator of Wnt signaling. *Proc. Natl. Acad. Sci. U.S.A.* 2008; 105:15417–15422. [PubMed: 18824696]
29. Thatcher EJ, Paydar I, Anderson KK, Patton JG. Regulation of zebrafish fin regeneration by microRNAs. *Proc. Natl. Acad. Sci. U.S.A.* 2008; 105:18384–18389. [PubMed: 19015519]
30. Bommer GT, Gerin I, Feng Y, Kaczorowski AJ, Kuick R, Love RE, Zhai Y, Giordano TJ, Qin ZS, Moore BB, MacDougald OA, Cho KR, Fearon ER. p53-mediated activation of miRNA34 candidate tumor-suppressor genes. *Curr. Biol*. 2007; 17:1298–1307. [PubMed: 17656095]
31. Chang TC, Wentzel EA, Kent OA, Ramachandran K, Mullendore M, Lee KH, Feldmann G, Yamakuchi M, Ferlito M, Lowenstein CJ, Arking DE, Beer MA, Maitra A, Mendell JT. Transactivation of miR-34a by p53 broadly influences gene expression and promotes apoptosis. *Mol. Cell*. 2007; 26:745–752. [PubMed: 17540599]
32. He L, He X, Lim LP, de Stanchina E, Xuan Z, Liang Y, Xue W, Zender L, Magnus J, Ridzon D, Jackson AL, Linsley PS, Chen C, Lowe SW, Cleary MA, Hannon GJ. A microRNA component of the p53 tumour suppressor network. *Nature*. 2007; 447:1130–1134. [PubMed: 17554337]
33. Yamakuchi M, Ferlito M, Lowenstein CJ. miR-34a repression of SIRT1 regulates apoptosis. *Proc. Natl. Acad. Sci. U.S.A.* 2008; 105:13421–13426. [PubMed: 18755897]
34. Attiyeh EF, London WB, Mosse YP, Wang Q, Winter C, Khazi D, McGrady PW, Seeger RC, Look AT, Shimada H, Brodeur GM, Cohn SL, Matthay KK, Maris JM. Chromosome 1p and 11q deletions and outcome in neuroblastoma. *N. Engl. J. Med.* 2005; 353:2243–2253. [PubMed: 16306521]
35. Bale SJ, Dracopoli NC, Tucker MA, Clark WH Jr, Fraser MC, Stanger BZ, Green P, Donis-Keller H, Housman DE, Greene MH. Mapping the gene for hereditary cutaneous malignant melanoma-dysplastic nevus to chromosome 1p. *N. Engl. J. Med.* 1989; 320:1367–1372. [PubMed: 2716782]
36. Calin GA, Sevignani C, Dumitru CD, Hyslop T, Noch E, Yendamuri S, Shimizu M, Rattan S, Bullrich F, Negrini M, Croce CM. Human microRNA genes are frequently located at fragile sites and genomic regions involved in cancers. *Proc. Natl. Acad. Sci. U.S.A.* 2004; 101:2999–3004. [PubMed: 14973191]
37. Lodygin D, Tarasov V, Epanchintsev A, Berking C, Knyazeva T, Korner H, Knyazev P, Diebold J, Hermeking H. Inactivation of miR-34a by aberrant CpG methylation in multiple types of cancer. *Cell Cycle*. 2008; 7:2591–2600. [PubMed: 18719384]
38. Tanaka K, Yanoshita R, Konishi M, Oshimura M, Maeda Y, Mori T, Miyaki M. Suppression of tumorigenicity in human colon carcinoma cells by introduction of normal chromosome 1p36 region. *Oncogene*. 1993; 8:2253–2258. [PubMed: 8101648]
39. Toyota M, Suzuki H, Sasaki Y, Maruyama R, Imai K, Shinomura Y, Tokino T. Epigenetic silencing of microRNA-34b/c and B-cell translocation gene 4 is associated with CpG island methylation in colorectal cancer. *Cancer Res*. 2008; 68:4123–4132. [PubMed: 18519671]
40. Miller LD, Smeds J, George J, Vega VB, Vergara L, Ploner A, Pawitan Y, Hall P, Klaar S, Liu ET, Bergh J. An expression signature for p53 status in human breast cancer predicts mutation status, transcriptional effects, and patient survival. *Proc. Natl. Acad. Sci. U.S.A.* 2005; 102:13550–13555. [PubMed: 16141321]
41. van de Wetering M, Sancho E, Verweij C, de Lau W, Oving I, Hurlstone A, van der Horn K, Batlle E, Coudreuse D, Haramis AP, Tjon-Pon-Fong M, Moerer P, van den Born M, Soete G, Pals S, Eilers M, Medema R, Clevers H. The beta-catenin/TCF-4 complex imposes a crypt progenitor phenotype on colorectal cancer cells. *Cell*. 2002; 111:241–250. [PubMed: 12408868]
42. Welch C, Chen Y, Stallings RL. MicroRNA-34a functions as a potential tumor suppressor by inducing apoptosis in neuroblastoma cells. *Oncogene*. 2007; 26:5017–5022. [PubMed: 17297439]

43. Lastowska M, Viprey V, Santibanez-Koref M, Wappler I, Peters H, Cullinane C, Roberts P, Hall AG, Tweddle DA, Pearson AD, Lewis I, Burchill SA, Jackson MS. Identification of candidate genes involved in neuroblastoma progression by combining genomic and expression microarrays with survival data. *Oncogene*. 2007; 26:7432–7444. [PubMed: 17533364]
44. Lee I, Ajay SS, Yook JI, Kim HS, Hong SH, Kim NH, Dhanasekaran SM, Chinnaiyan AM, Athey BD. New class of microRNA targets containing simultaneous 5'-UTR and 3'-UTR interaction sites. *Genome Res*. 2009; 19:1175–1183. [PubMed: 19336450]
45. Bessard AC, Garay E, Lacroinque V, Legros Y, Demarquay C, Houque A, Portefaix JM, Granier C, Soussi T. Regulation of the specific DNA binding activity of *Xenopus laevis* p53: evidence for conserved regulation through the carboxy-terminus of the protein. *Oncogene*. 1998; 16:883–890. [PubMed: 9484779]
46. Funayama N, Fagotto F, McCrean P, Gumbiner BM. Embryonic axis induction by the armadillo repeat domain of beta-catenin: evidence for intracellular signaling. *J. Cell Biol*. 1995; 128:959–968. [PubMed: 7876319]
47. Morin PJ, Sparks AB, Korinek V, Barker N, Clevers H, Vogelstein B, Kinzler KW. Activation of beta-catenin-Tcf signaling in colon cancer by mutations in beta-catenin or APC. *Science*. 1997; 275:1787–1790. [PubMed: 9065402]
48. Fearon ER, Vogelstein B. A genetic model for colorectal tumorigenesis. *Cell*. 1990; 61:759–767. [PubMed: 2188735]
49. Ota I, Li XY, Hu Y, Weiss SJ. Induction of a MT1-MMP and MT2-MMP-dependent basement membrane transmigration program in cancer cells by Snail1. *Proc. Natl. Acad. Sci. U.S.A.* 2009; 106:20318–20323. [PubMed: 19915148]
50. Knudson AG Jr. Mutation and cancer: statistical study of retinoblastoma. *Proc. Natl. Acad. Sci. U.S.A.* 1971; 68:820–823. [PubMed: 5279523]
51. Mayr C, Bartel DP. Widespread shortening of 3'UTRs by alternative cleavage and polyadenylation activates oncogenes in cancer cells. *Cell*. 2009; 138:673–684. [PubMed: 19703394]
52. Thiele A, Nagamine Y, Hauschildt S, Clevers H. AU-rich elements and alternative splicing in the beta-catenin 3'UTR can influence the human beta-catenin mRNA stability. *Exp. Cell Res*. 2006; 312:2367–2378. [PubMed: 16696969]
53. Molchadsky A, Shats I, Goldfinger N, Pevsner-Fischer M, Olson M, Rinon A, Tzahor E, Lozano G, Zipori D, Sarig R, Rotter V. p53 plays a role in mesenchymal differentiation programs, in a cell fate dependent manner. *PLoS One*. 2008; 3:e3707. [PubMed: 19002260]
54. Jernigan KK, Cselenyi Cs, Thorne CA, Hanson AJ, Tahinci E, Hajicek N, Oldham WM, Lee LA, Hamm HE, Helper JR, Kozasa T, Linder ME, Lee E. Gβγ activates GSK3 to promote LRP6-mediated β-catenin transcriptional activity. *Sci Signal*. 2010; 3:ra37. [PubMed: 20460648]
55. Wan M, Li J, Herbst K, Zhang J, Yu B, Wu X, Qiu T, Lei W, Lindvall C, Williams BO, Ma H, Zhang F, Cao X. LRP6 mediates cAMP generation by G protein-coupled receptors through regulating the membrane targeting of Gαs. *Sci. Signal*. 2011; 4:ra15. [PubMed: 21406690]
56. Hashimi ST, Fulcher JA, Chang MH, Gov L, Wang S, Lee B. MicroRNA profiling identifies miR-34a and miR-21 and their target genes JAG1 and WNT1 in the coordinate regulation of dendritic cell differentiation. *Blood*. 2009; 114:404–414. [PubMed: 19398721]
57. Kim NH, Kim HS, Li X-Y, Lee I, Choi H-S, Kang SE, Cha SY, Ryu JK, Yoon D, Fearon ER, Rowe RG, Lee S, Maher CA, Weiss SJ, Yook JI. A p53/miRNA-34 axis regulates Snail1-dependent cancer cell epithelial-mesenchymal transition. *J. Cell Biol*. in press.
58. Chang CJ, Chao CH, Xia W, Yang JY, Xiong Y, Li CW, Yu WH, Rehman SK, Hsu JL, Lee HH, Liu M, Chen CT, Yu D, Hung MC. p53 regulates epithelial-mesenchymal transition and stem cell properties through modulating miRNAs. *Nat. Cell Biol*. 2011; 3:317–312. [PubMed: 21336307]
59. Burk U, Schubert J, Wellner U, Schmalhofer O, Vincan E, Spaderna S, Brabletz T. A reciprocal repression between ZEB1 and members of the miR-200 family promotes EMT and invasion in cancer cells. *EMBO Rep*. 2008; 9:582–589. [PubMed: 18483486]
60. Saydam O, Shen Y, Wurdinger T, Senol O, Boke E, James MF, Tannous BA, Stemmer-Rachamimov AO, Yi M, Stephens RM, Fraefel C, Gusella JF, Krichevsky AM, Breakefield XO. Downregulated microRNA-200a in meningiomas promotes tumor growth by reducing E-cadherin

- and activating the Wnt/beta-catenin signaling pathway. *Mol. Cell Biol.* 2009; 29:5923–5940. [PubMed: 19703993]
61. Eliyahu D, Michalovitz D, Eliyahu S, Pinhasi-Kimhi O, Oren M. Wild-type p53 can inhibit oncogene-mediated focus formation. *Proc. Natl. Acad. Sci. U.S.A.* 1989; 86:8763–8767. [PubMed: 2530586]
  62. He TC, Sparks AB, Rago C, Hermeking H, Zawel L, da Costa LT, Morin PJ, Vogelstein B, Kinzler KW. Identification of c-MYC as a target of the APC pathway. *Science.* 1998; 281:1509–1512. [PubMed: 9727977]
  63. Wei JS, Song YK, Durinck S, Chen QR, Cheuk AT, Tsang P, Zhang Q, Thiele CJ, Slack A, Shohet J, Khan J. The MYCN oncogene is a direct target of miR-34a. *Oncogene.* 2008; 27:5204–5213. [PubMed: 18504438]
  64. Cicalese A, Bonizzi G, Pasi CE, Faretta M, Ronzoni S, Giulini B, Brisken C, Minucci S, Di Fiore PP, Pelicci PG. The tumor suppressor p53 regulates polarity of self-renewing divisions in mammary stem cells. *Cell.* 2009; 138:1083–1095. [PubMed: 19766563]
  65. Schwab M, Pram L, Amler LC. Genomic instability in 1p and human malignancies. *Genes Chromosomes Cancer.* 1996; 16:211–229. [PubMed: 8875235]
  66. Watanabe T, Nakamura M, Cros JM, Burkhard C, Yonekawa Y, Leihues P, Ohgaki H. Phenotype versus genotype correlation in oligodendrogliomas and low-grade diffuse astrocytomas. *Acta. Neuropathol.* 2002; 103:267–275. [PubMed: 11907807]
  67. Thon N, Eigenbrod S, Grasbon-Frodl EM, Rüter M, Mehrkens JH, Kreth S, Tonn JC, Kretschmar HA, Kreth FW. Novel molecular stereotactic biopsy procedures reveal intratumoral homogeneity of loss of heterozygosity of 1p/19q and TP53 mutations in World Health Organization grade II gliomas. *J. Neuropathol. Exp. Neurol.* 2009; 68:1219–1228. [PubMed: 19816195]
  68. Kim KH, Park TK, Yoon DJ, Kim YS. The effects of wild type p53 tumor suppressor gene expression on the normal human cervical epithelial cells or human epidermal keratinocytes transformed with human papillomavirus type 16 DNA. *Yonsei Med. J.* 1995; 36:287–298. [PubMed: 7660680]
  69. Brummelkamp TR, Bernards R, Agami R. A system for stable expression of short interfering RNAs in mammalian cells. *Science.* 2002; 296:550–553. [PubMed: 11910072]

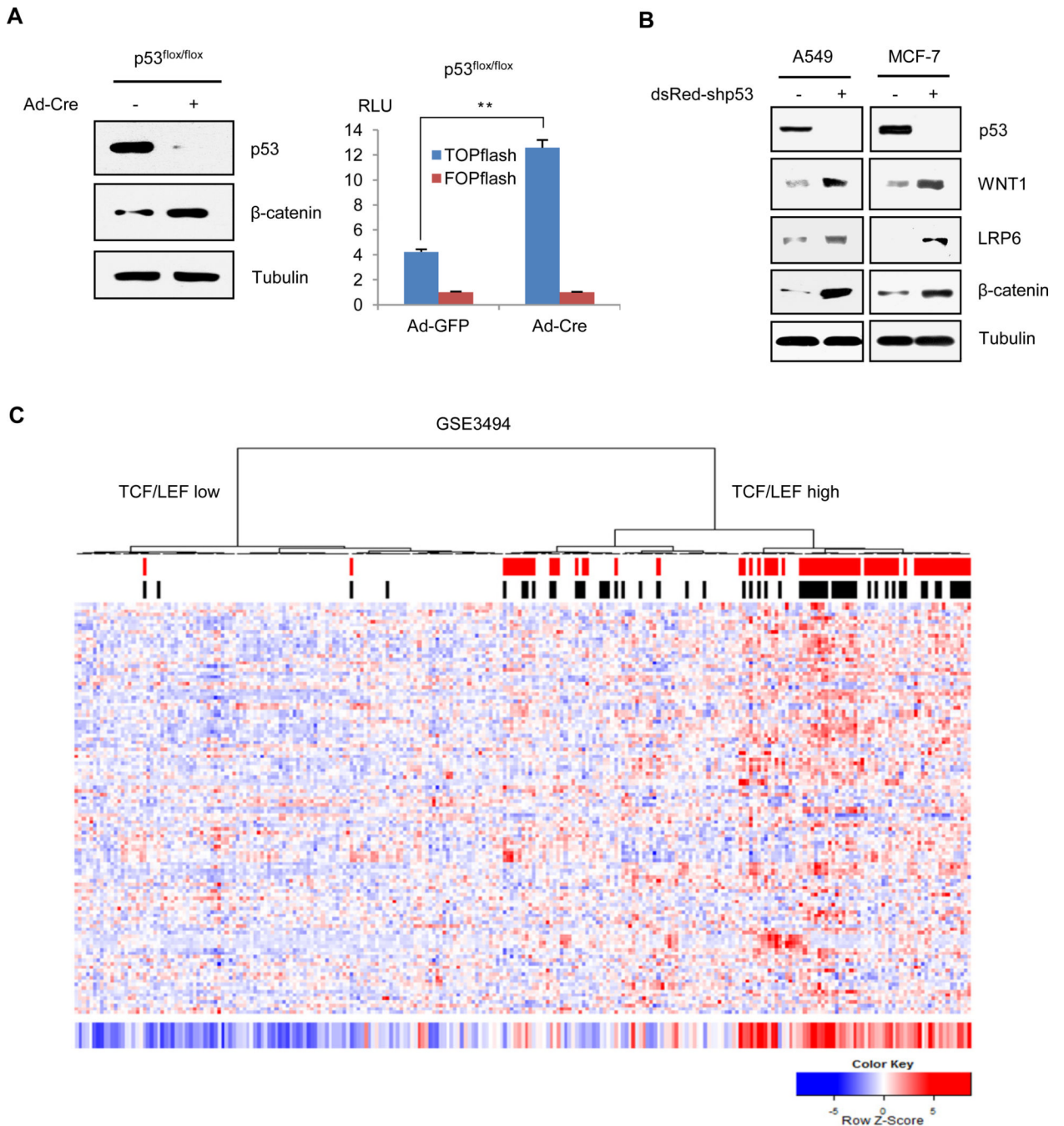


**Fig. 1.** Loss of p53 function potentiates Wnt activity in cells and samples of breast cancer tissue. **(A)** Immunoblot analysis of  $\beta$ -catenin (left panels,  $n = 2$ ) and TOPflash activities (right panel) following Cre recombinase-mediated deletion of wt-p53 in  $p53^{\text{flox/flox}}$  MEFs. TOPflash and FOPflash activities were normalized to a co-transfected SV-40-*Renilla* and relative changes in relative light units (RLU) was represented ( $n = 3$ , error bars, standard deviation,  $**P < 0.01$ ). **(B)** Immunoblot analysis of WNT1, LRP6, and  $\beta$ -catenin following knock-down of wt-p53 in A549 or MCF-7 cells ( $n = 2$ ). **(C)** Unsupervised hierarchical clustering of breast cancer cohort using a TCF/LEF gene signature to distinguish between

subsets of tumors with mutant p53 function (red bars, Fisher exact test  $P = 1.19E-22$ ) as well as p53 cDNA mutation status (black bars, Fisher exact test  $P = 4.59E-14$ ). The Uppsala breast cancer specimens (GSE3494,  $n = 251$ ) were clustered (columns) using genes responsive to dominant-negative TCF. In the heatmap, red denotes higher relative expression whereas blue indicates lower relative expression, with degree of color saturation reflecting the magnitude of the log expression signal. The bottom row represents the median log expression value of TCF/LEF target genes.

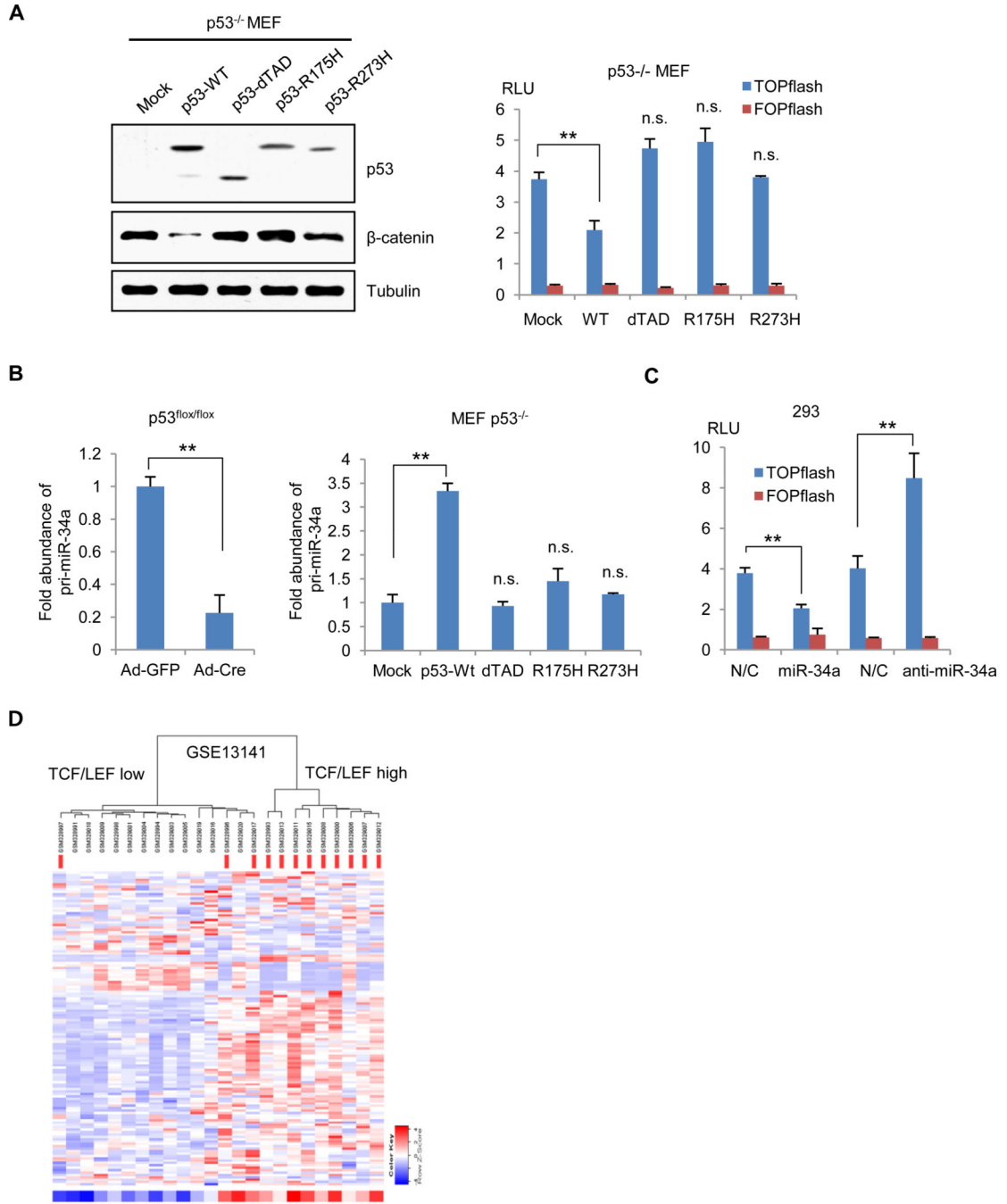


**Fig. 2.** p53 represses Wnt activity via miR-34 transactivation. (A) Immunoblot analysis of β-catenin (left panels) and TCF/LEF activities (right panel, n = 2) following stable transduction with a control (Mock) or various p53-expressing lentiviruses in p53<sup>-/-</sup> MEFs (n = 3, \*\*P < 0.01, n.s., not significant). (B) pri-miR-34a expression was determined by quantitative RT-PCR following p53 deletion by Cre-recombinase (left panel, n = 2) or stable transduction with a control or various wt or mutant p53-expressing lentiviruses in p53<sup>-/-</sup> MEFs (right panel). Relative fold change of pri-miR-34a abundance was statistically significant compared to control (n = 3, \*\*P < 0.01). (C) Wnt transcriptional activity was

inhibited by miR-34a, and potentiated by the inhibition of miR-34a in HEK293 cells ( $n = 3$ ,  $**P < 0.01$ ). TOPflash (blue) and FOPflash (red) luciferase expression vectors were co-transfected with negative control miR (N/C), synthetic miR-34a precursor (miR-34a), or inhibitor (anti-miR-34a) in HEK293 cells. **(D)** Unsupervised hierarchical clustering of pediatric neuroblastoma samples (GSE13141) using a TCF/LEF signature segregates a subset of tumors with chromosomal loss of miR-34a (Fisher exact test  $P = 0.000033$ ). Red bars represent patient samples with 1p loss. The bottom row denotes the median log expression value of TCF/LEF target genes.

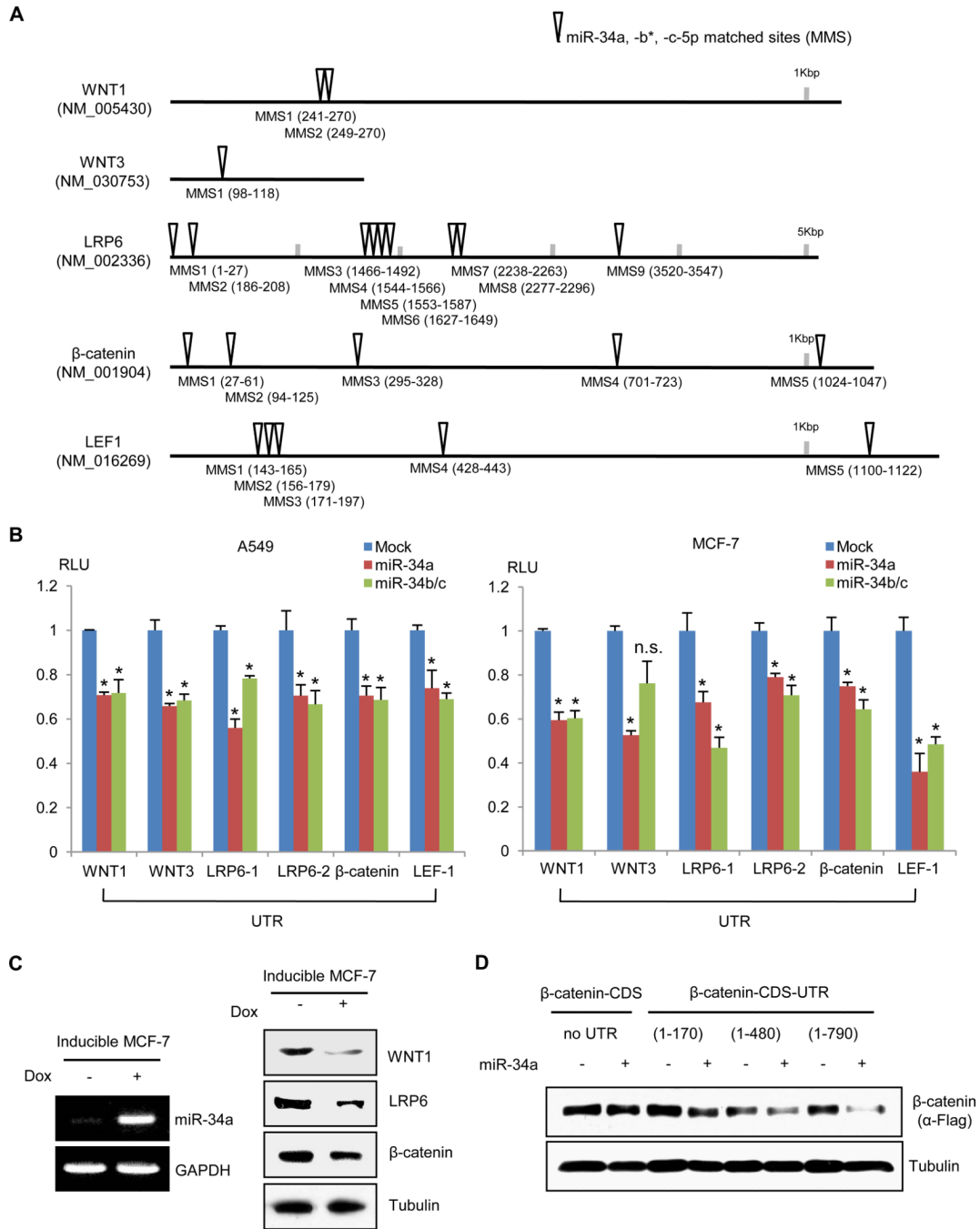


**Fig. 3.** The miR-34 family directly targets the UTR of genes involved in the canonical Wnt pathway. (A) Potential matching target sites of the miR-34a family in the 3' UTR of WNT1, WNT3, LRP6,  $\beta$ -catenin, and LEF1. Predicted matching sites of miR-34a, -34b\* and -34c-5p are denoted as miR-matched sites (MMS; open arrow heads). (B) Reporter constructs in which Wnt gene UTRs were cloned downstream of firefly luciferase were transfected into A549 (left panel) or MCF-7 cells (right panel) with control (Mock) or miR-34 family expression vectors. Relative luciferase activity in comparison to the non-UTR control reporter are shown (27); the error bar represents the standard deviation (n = 3,

\* $P < 0.05$ ; n.s., not significant compared to each control). (C) RT-PCR (left panels) and immunoblot analysis (n = 2, right panels) of pri-miR-34a and Wnt-pathway proteins following treatment with doxycycline (0.5  $\mu\text{g/ml}$ ) for a 24 h period in miR-34a-inducible MCF-7 cells. (D) Immunoblot analysis of HEK293 cells transfected with a Flag-tagged  $\beta$ -catenin cDNA expression vector without its UTR ( $\beta$ -catenin-CDS) or with cDNA expression vectors harboring different lengths of the  $\beta$ -catenin UTR (+1 to 170, +1 to 480, +1 to 790, n = 2).

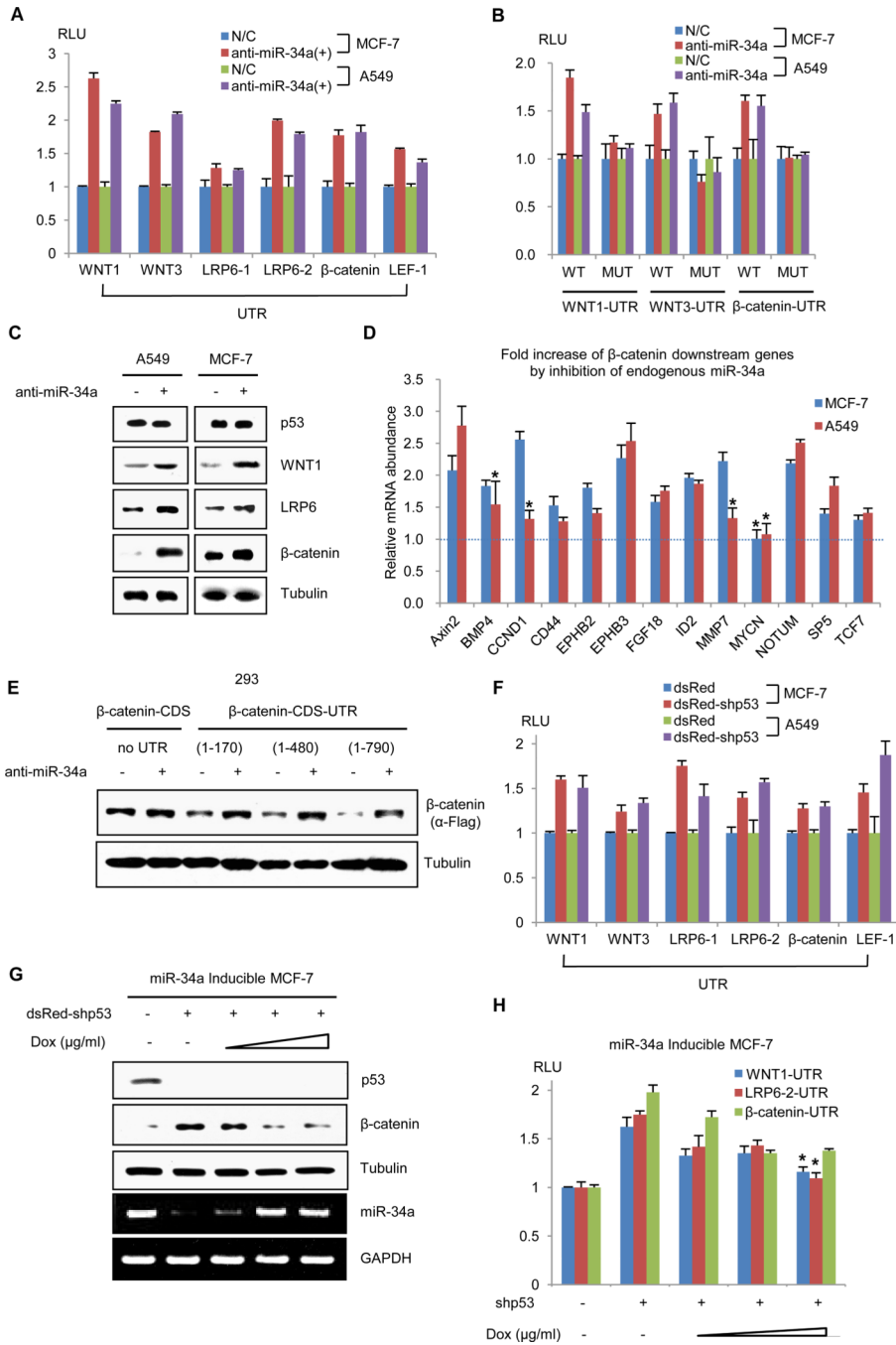


**Fig. 4.** Functional activity of endogenous miR-34. **(A)** Transduction of anti-miR-34a (+) increased each UTR activities relative to that of the negative control (N/C). All results were statistically significant compared to respective control by *t* test;  $P < 0.05$ . **(B)** The relative wt and mutant UTR activities. **(C)** Immunoblot of WNT1, LRP6, or  $\beta$ -catenin abundance following transduction of control (-) or anti-miR-34a (+) in A549 or MCF-7 cells ( $n = 2$ ). **(D)** Quantitative RT-PCR analysis of  $\beta$ -catenin target genes in anti-miR-34a-transfected cells ( $n = 3$ ); \* $P > 0.05$ , not significant. **(E)** Immunoblot analysis ( $n = 2$ ) of  $\beta$ -catenin expression vectors with or without UTR following transduction of negative control (-) or

anti-miR-34a (+). **(F)** The UTR reporter activities by knock-down of p53 (dsRed-shp53) relative to the negative control (dsRed); n = 3,  $P < 0.05$ . **(G)** Immunoblot (upper, n = 2) of  $\beta$ -catenin and RT-PCR (lower, n = 2) of pri-miR-34a abundance transduced with dsRed vector control (-) or with knock-down of p53 (dsRed-shp53). Pri-miR-34a expression was induced by treatment with doxycycline (0.125, 0.25, 0.5  $\mu\text{g/ml}$ ) for 24 h. **(H)** Wnt UTR reporter activity following induction of miR-34a (n = 3). \* $P > 0.05$ , not significant compared to shp53-, Dox-.

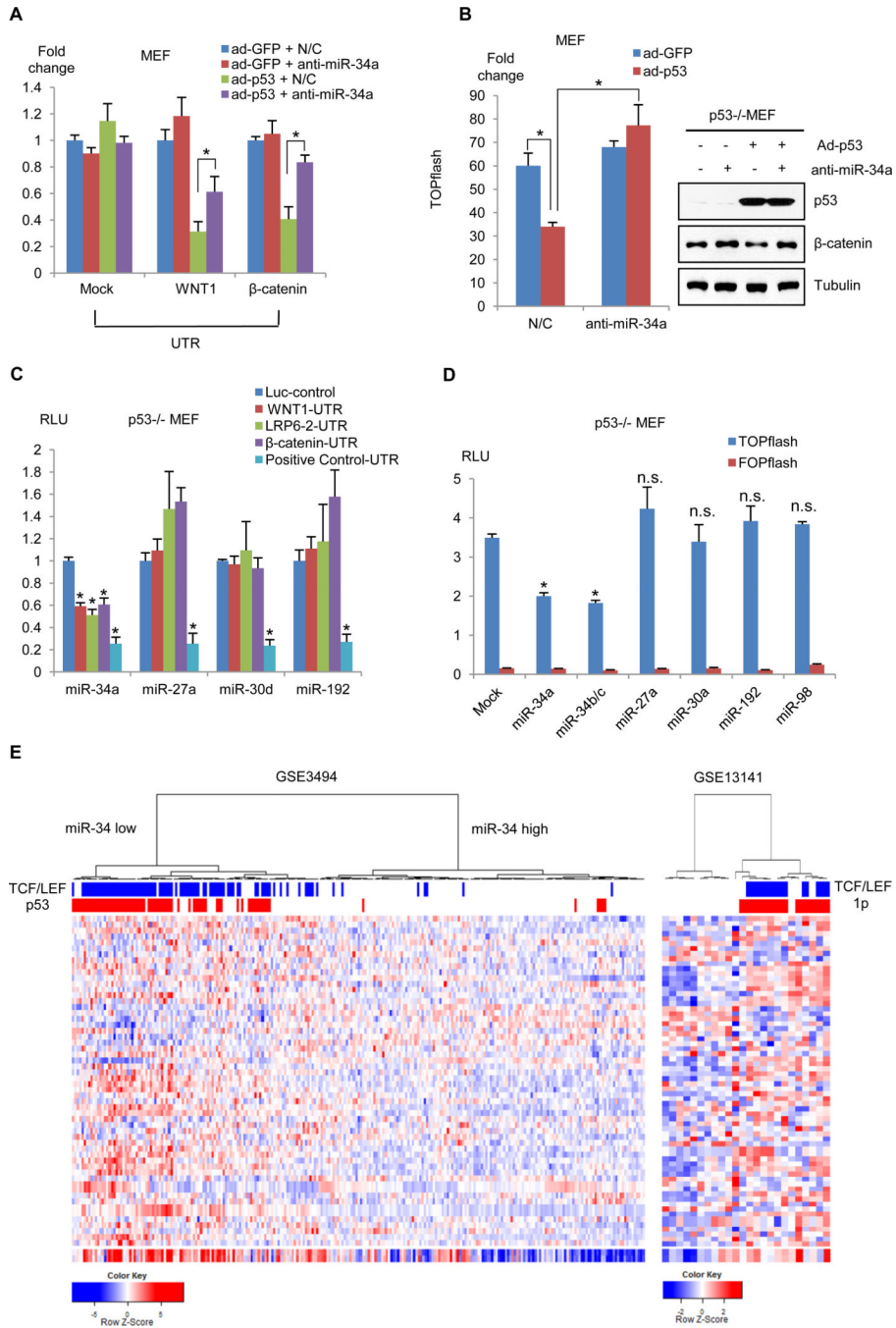


**Fig. 5.** Endogenous miR-34 mediates p53-dependent inhibition of TCF/LEF target genes. **(A)** Activity of Wnt pathway reporter genes was inhibited following transduction of wt-p53, and this inhibition was reversed by deletion of miR-34a ( $n = 3$ ,  $*P < 0.01$ ). **(B)** p53-dependent decrease in TOPflash activity (left panel) and  $\beta$ -catenin abundance (right panels) were relieved by depleting miR-34a ( $*P < 0.01$ ). **(C and D)** UTR reporter for Wnt-pathway genes (C) and TOPflash (D) were co-expressed with miRNA expression vectors as indicated and the relative expression of luciferase determined ( $*P < 0.01$ , one-sided  $t$  test). **(E)** Hierarchical clustering of breast cancer (GSE3494, left panel) or neuroblastoma

(GSE13141, right panel) samples using a miR-34 signature (32). Hierarchical clustering of clinical samples with miR-34 signature associated with a subset of tumors with high TCF/LEF activity and defects in p53 functionality in breast cancer ( $P= 1.20E-29$  in TCF/LEF activity,  $P= 1.60E-24$  in p53 function) or 1p deletion in neuroblastoma ( $P= 0.002$  in TCF/LEF activity,  $P= 6.73E-05$  in 1p-deletion), respectively. Blue bars represent patient samples with a high TCF/LEF subset in Fig. 1C and Fig. 2D, and red bars represent mutant p53 function or 1p-deleted samples. The bottom row denotes the median expression value ( $\log_2$ ) of miR-34 responsive genes.

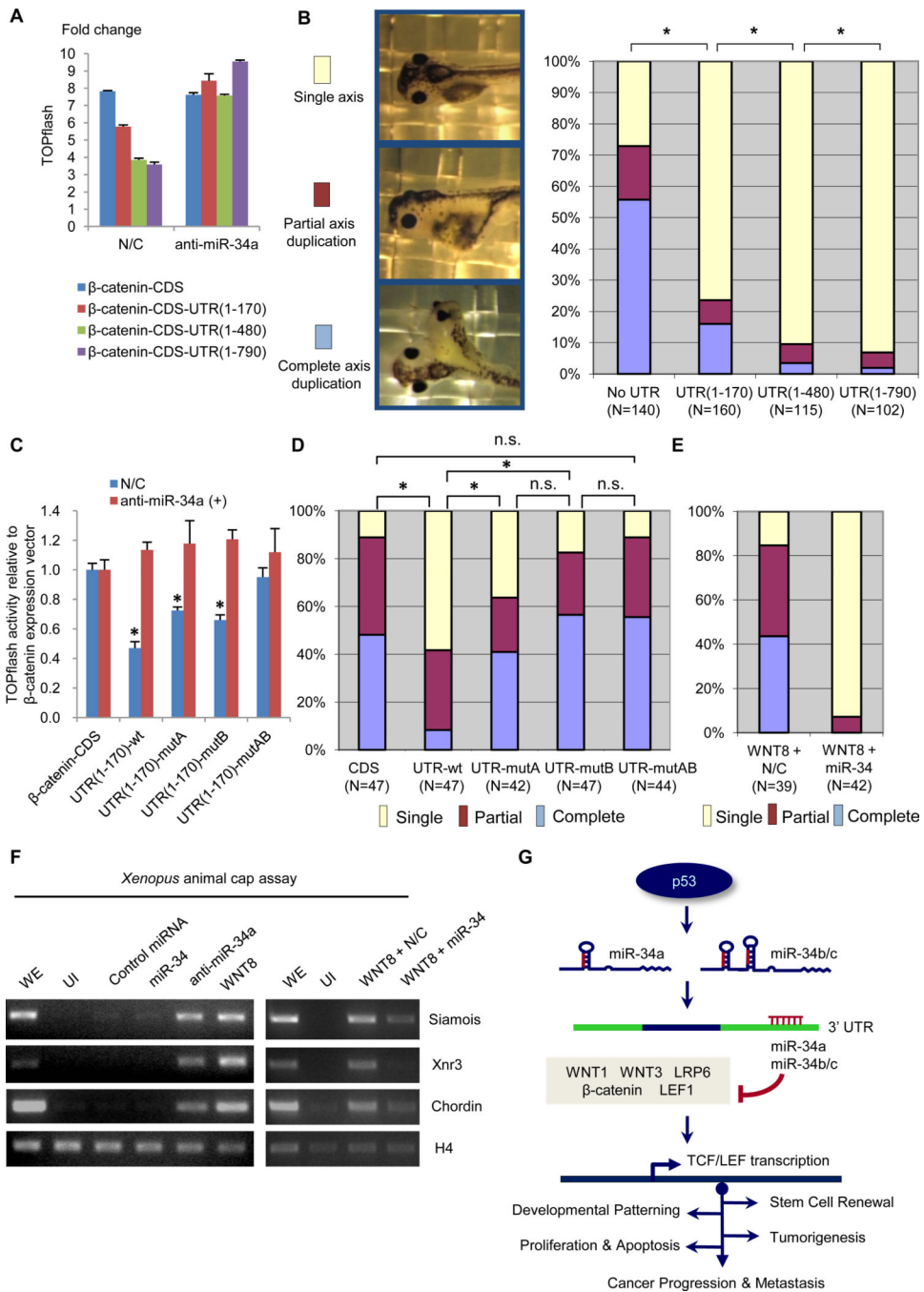


**Fig. 6.** Specific interactions between miR-34 and the  $\beta$ -catenin UTR regulate the Wnt pathway during *Xenopus* development. **(A)** TOPflash activities of wild type  $\beta$ -catenin expression vectors harboring variable UTR lengths with negative control (N/C) or synthetic miR-34a inhibitor (anit-miR-34a) in HEK293 cells ( $*P < 0.01$ ). **(B)** Axis duplication by  $\beta$ -catenin during *Xenopus* development is blocked by miR-UTR interaction. *Xenopus* embryos was injected with 30 pg of  $\beta$ -catenin mRNA either without a UTR or with variable-sized UTRs and embryos were scored as described in Methods;  $*P < 0.05$ . **(C and D)** TOPflash activity in 293 cells (C) and *Xenopus* axis duplication (D) by  $\beta$ -catenin depends on miR-34-UTR

interactions (\* $P < 0.01$ ; n.s., not significant). (E) Wnt8 mRNAs were co-injected with control miR (N/C) or miR-34 into one of the ventral vegetal blastomeres of 4- to 8-cell-stage embryos,  $P < 0.01$ . (F) Induction or repression of Wnt/ $\beta$ -catenin target patterning genes in *Xenopus laevis* animal cap explants by respectively depleting miR-34a levels (left panels) or supplementing miR-34a levels with Wnt8 (right panels). Fertilized 2-cell stage embryos were injected with indicated miRs, and animal caps for RT-PCR analysis were performed as described in Methods. *Xenopus* histone H4, loading control. Lanes: WE, whole embryo; UI, un-injected. (G) Schematic diagram of p53-mediated inhibition of canonical Wnt signaling.

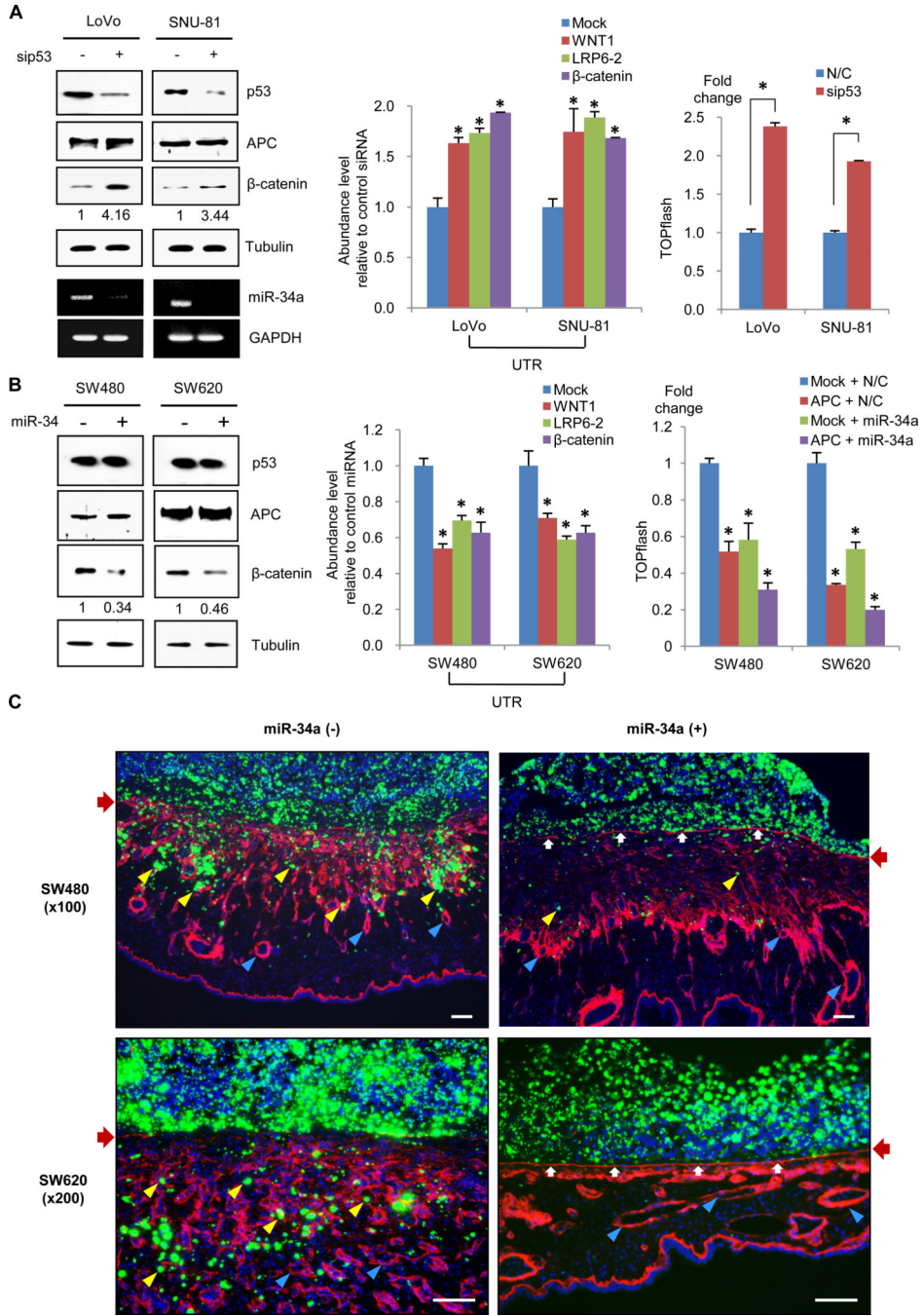


**Fig. 7.** Loss of p53/miR-34 function augments canonical Wnt activity and triggers a tissue-invasive phenotype in colorectal cancer cells. **(A)** p53 knockdown increased  $\beta$ -catenin abundance (relative fold abundance reported below the blot,  $n = 2$ ), leaving truncated APC abundance unaltered (left panels). Wnt UTR (middle panel,  $*P < 0.01$ ) and TOPflash (right panel,  $*P < 0.01$ ) activities were measured following knock-down of p53 in APC-mutant colorectal cancer cells with wt-p53 function. **(B)** Transduction of mature miR-34a decreased  $\beta$ -catenin abundance (left panels,  $n = 2$ ) and Wnt UTR activities (middle panel). Co-transfection with an APC expression vector and miR-34a additively, and independently, repressed TOPflash

activities in colorectal cancer cells (right panel,  $*P < 0.01$  compared to control). (C) Negative control (-) or miR-34a (+) transduced SW480 or SW620 cells were cultured atop the embryonic chick CAM (upper CAM surface demarcated by red arrows) and the invasive activity of cancer cells (labeled with green fluorescent beads) was monitored by fluorescence microscopy. Yellow arrowheads indicate invading cancer cells. White arrows and blue arrowheads denote the basement membrane of the upper CAM and blood vessels in interstitial CAM tissues, respectively. Bar, 100  $\mu\text{m}$ .